An Optimized Maximum Power Point Tracking Method Based on PV Surface Temperature Measurement

Roberto Francisco Coelho and Denizar Cruz Martins

Additional information is available at the end of the chapter

http://dx.doi.org/10.5772/51020

1. Introduction

On the last decades, distributed generation (DG) systems based on photovoltaic (PV) generation are slowly been introduced to the world energy matrix, in which some important aspects as political incentive, cost reduction, electricity rising demand, improvements on PV materials and increasing on power converters efficiency have contributed to the present scenario [1-3].

From the power processing point of view, high efficiency conversion, by itself, cannot ensure the optimized power flow, since the PV output voltage and current are strongly dependent on environmental conditions, i.e., solar radiation and temperature; however, on the literature, many works bring solutions to maximize the photovoltaic output power, employing specific circuits denominated by Maximum Power Point Trackers (MPPT) [4-8]. In most applications, the MPPT is a simple dc-dc converter interposed between the photovoltaic modules and the load, and its control is achieved through a tracking algorithm.

The studies on the MPPT area are normally grouped in two categories: the first one relates to the dc-dc converter topology optimization, focusing on methods to determine a suitable dc-dc converter for operating as MPPT [9]; and the second one refers to the maximum power point tracking algorithm, responsible for properly controlling the dc-dc converter in order to establish the system operating point as close as possible to the Maximum Power Point (MPP). Therefore, an *efficient* MPPT system need to be composed by the integration of an adequate dc-dc converter (hardware) and proper tracking algorithm (software), resulting in some desired aspects:

- Fast tracking response (dynamic analysis);

- Accuracy and no oscillation around the MPP (stead-state analysis);

- Capacity to track the MPP for wide ranges of solar radiation and temperature;

- Simplicity of implementation;

- Low cost.

The most popular algorithms employed in PV tracking systems [10-18] - Constant Voltage, Perturb and Observe (P&O) and Incremental Conductance (IncCond) – are extensively explored by specialized literature, nevertheless, since fast tracking response and accuracy conflict one from other, the mentioned tracking methods cannot satisfy, simultaneously, both of them. In place of the traditional and spread methods, some authors have proposed complex MPPT algorithms, based on fuzzy logic and neural network, in order to accomplish fast tracking response and accuracy in a single system. These proposals, nevertheless, present some disadvantageous: needed for high processing capacity, complexity, cost elevation and, in some cases, employment of extra sensors.

In this chapter, PV maximum power point tracking systems are analyzed under two distinct points of view: firstly, the influence of the dc-dc converter on the tracking quality is accounted. In this study, the effect of solar radiation, temperature and load variations are considered, and the tracking performance of Buck, Boost, Buck-Boost, Cuk, SEPIC and Zeta converters are compared. Secondly, a new tracking algorithm, based on the PV surface temperature, is introduced. The advantages concerning the proposed method come from the simplicity, low cost, analogue or digital implementation, fast tracking response, accuracy and no oscillation around the MPP on steady state.

In order to achieve the main chapter topics, a brief revision of PV generation is highlighted in next section.

2. Photovoltaic Generation

Photovoltaic modules output power depends on environmental conditions, such as solar radiation and temperature, resulting in a non-liner and time-variant power source. The employment of a PV generator only can be successfully attained if it is correctly characterized.

2.1. Relationship Among PV Cell, Module and Array

Photovoltaic cells are the basic building blocks on construction of PV power systems. The amount of power delivered by a PV cell is, typically, restricted to few Watts, due to the surface area limitation. For raising the generated power, in order to reach hundreds of Watts, PV cells may be grouped in a PV module. Similarly, it is possible to connect a group of PV modules (series, parallel or both) in order to obtain a PV array, whose power range is established from kilo-Watts to mega-Watts [19]. The distinction among PV cell, module and array is illustrated at Figure 1.
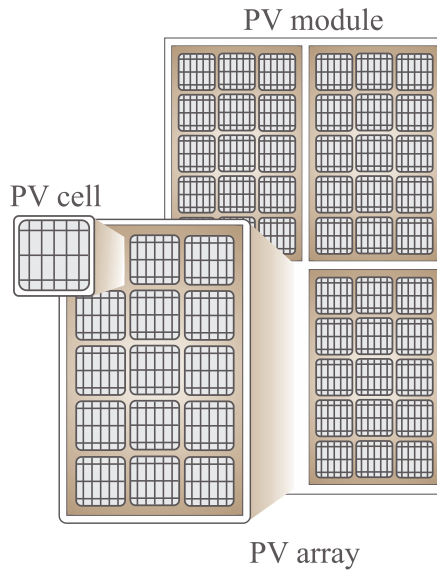
Figure 1. PV array composed by an arrangement of PV modules and PV module composed by an arrangement of PV cells.

2.1.1. Standard Test Condition

The Standard Test Conditions (STC) refers to the conditions under which PV modules are tested in laboratory. STC defines the values of irradiance, temperature and air mass index, in which the manufactures feature the PV devices, permitting to compare their performance and efficiency conversion.

2.1.2. Irradiance

The Sun energy reaches to the Earth through electromagnetic waves, resulting in an irradiance (or solar radiation) of about 1366 W/m^2 on its outer atmosphere. However, due to atmospheric effects – scattering, absorption and reflection -, the incoming irradiance is modified before reaching the Earth's surface [20].

The process of scattering occurs when small particles and gas molecules diffuse the radiation in random directions, while absorption is defined as a process in which the solar radiation is retained by atmosphere substances and converted into heat. In addition, part of the total solar radiation is redirected back to the space by reflection and part, termed by direct

solar radiation, reaches the Earth's surface unmodified by any of the above atmospheric processes, as depicts Figure 2.
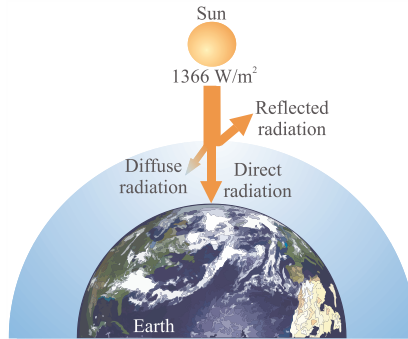

Figure 2. Atmosphere effects on incoming solar radiation.

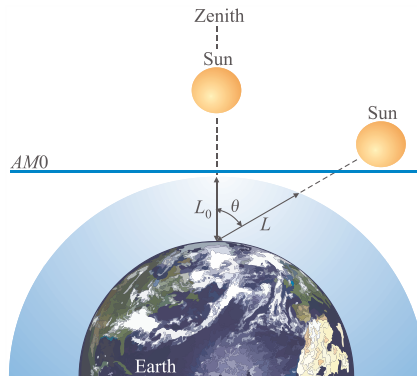Since the direct radiation on a clear day, at noon, is typically 1000 W/m², this value is adopted as reference at STC.

Figure 3. Solar radiation path across the Earth's atmosphere.

2.1.3. Air Mass

The Air Mass (*AM*) index quantify the solar radiation path (*L*) across the atmosphere, normalized by the shorter path (L_0), measured from the zenith angle, as is depicted in Figure 3 and mathematically described by (1) [19]. The index *AM*0 is used to describe the radiation path out of the atmosphere, where the irradiance is constant and equal to 1366 W/m².

$$AM = \frac{L}{L_0} = \frac{1}{\cos(\theta)} \tag{1}$$

On industry, PV modules are standardized considering an air mass index of AM=1.5. This value comes from a angle of aproximatly 48°, proper representing the PV instalitions around the most populed centres across Europe, China, Japan and United States of America, located in mid-latitudes. This value is also adopted as reference at STC.

2.1.4. Temperature

The third parameter used to characterize a PV module is its surface temperature. The STC temperature value adopted for PV modules characterization is T=25 °C.

2.2. I-V and P-V generation curves

Under the specified Standard Test Conditions, expressed by (2), PV modules are tested and featured by I-V (current versus voltage) and P-V (power versus voltage) curves, in which the effect of solar radiation and temperature on the PV generated power is evidenced.

$$
\begin{aligned}
S^{STC} &= 1000 \text{ W/m}^2 \\
T^{STC} &= 25 \text{ °C} \\
AM^{STC} &= 1.5
\end{aligned}
\tag{2}
$$

Although both, solar radiation and temperature, are strongly coupled, solar radiation predominantly influences the PV module output current, while temperature mainly changes the PV module output voltage, as depicts the I-V curve presented at Figure 4, obtained from Kyocera KC200GT PV module datasheet.

One of most important PV module operation point is obtained on the knee of the I-V curve. In this point, named by maximum power point (MPP), the product of the PV output voltage and current results at the maximum available power, for a given solar radiation and temperature. For emphasizing the maximum power point, an alternative P-V (power versus voltage) curve may be plotted, in accordance with Figure 5.

Mathematical expressions for calculating the PV module output voltage V_{mpp} and current I_{mpp} on MPP are given by (3) and (4), whose product results on the PV output power P_{mpp}, according to (5) [21], where:

V_{mpp}, I_{mpp}, P_{mpp} : PV module output voltage, current and power on MPP for any irradiance (S) and surface temperature (T);

V_{mpp}^{STC}, I_{mpp}^{STC}, P_{mpp}^{STC} : PV module output voltage, current and power on MPP. These parameters are obtained from datasheet and specified on STC (T^{STC} and S^{STC});

μ_V, μ_A : Temperature voltage coefficient (V/°C) and temperature current coefficient (A/°C). These parameters are also obtained from datasheet.

$$V_{mpp} = V_{mpp}^{STC} + \left(T - T^{STC}\right)\mu_V \tag{3}$$

$$I_{mpp} = \frac{S}{S^{STC}}I_{mpp}^{STC} + \left(T - T^{STC}\right)\mu_A \tag{4}$$

$$P_{mpp} = \frac{S}{S^{STC}}P_{mpp}^{STC} + \left(T - T^{STC}\right)\left(\frac{S}{S^{STC}}\mu_V I_{mpp}^{STC} + \mu_A V_{mpp}^{STC}\right) + \left(T - T^{STC}\right)^2\mu_V\mu_A \tag{5}$$

Note that (5) is useful once it allows estimating the amount of available PV power only from the environmental data (S, T). All other related parameters are commonly specified on PV module datasheet. For instance, considering the KC200GT PV module, the following datasheet specifications are found:
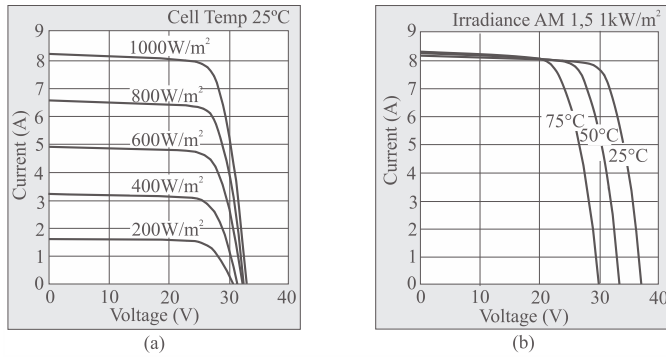

Figure 4. I-V curve from Kyocera KC200GT PV module: (a) under constant temperature and (b) under constant irradiance.

PV specified parameter	Value
V_{mpp}^{STC}	26.3 V
I_{mpp}^{STC}	7.61 A
P_{mpp}^{STC}	200 W
μ_V	-0.14 V/°C
μ_A	0.00318 A/°C

Table 1. PV module specifications on STC from Kyocera KC200GT PV module datasheet.

Furthermore, short circuit current (I_{sc}) and open circuit voltage (V_{oc}) are also important for a complete PV module characterization. They remark the points where the PV generated pow-

er is null, but the output current or voltage reach the maximum value, respectively. Figure 6 highlights I_{sc}, V_{oc}, I_{mpp}, V_{mpp} and P_{mpp} on both, I-V and P-V curves.
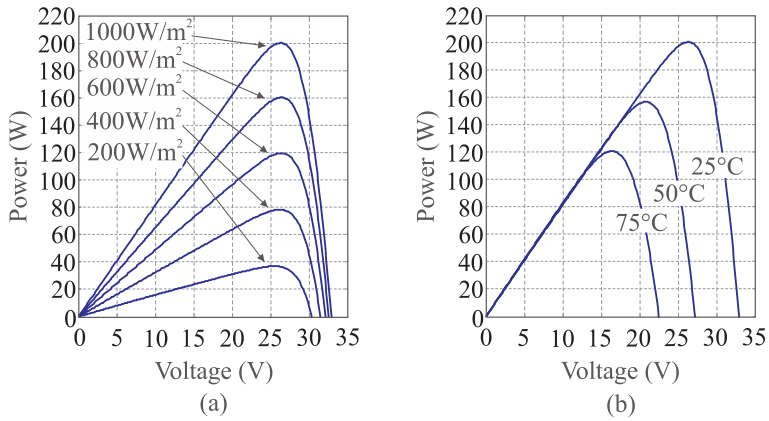

Figure 5. P-V curve from Kyocera KC200GT PV module obtained by simulation: (a) under constant temperature and (b) under constant solar radiation.
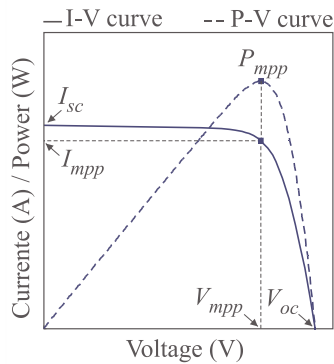

Figure 6. Identification of I_{sc}, V_{oc}, I_{mpp}, V_{mpp} and P_{mpp} on the I-V and P-V curves.

3. Maximum power point tracker

For maximizing the PV conversion efficiency, the incoming sun energy must be converted to electricity with the highest efficiency, accomplished when the photovoltaic module operates on the maximum power point. Nevertheless, since this operating point is strongly affected

by the solar radiation and temperature levels, it may randomly vary along the I-V plan, as illustrates Figure 7.
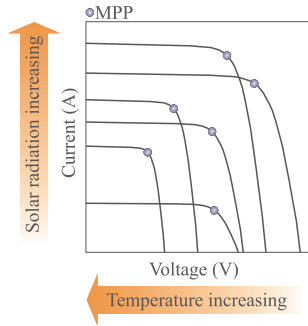

Figure 7. MPP across the I-V plan considering solar radiation and temperature changes.

Thus, in order to dynamically set the MPP as operation point for a wide range of solar radiation and temperature, specific circuits, known at the literature by Maximum Power Point Trackers (MPPT), are employed.

In this chapter the studies concerning MPPT are grouped in two categories: the first is related to hardware, in which the influence of the dc-dc converter and load-type on the tracking quality is investigated, and the second refers to the software, where tracking accuracy and speed are targeted.

3.1. MPPT from the dc-dc converter point of view

The operating point of a photovoltaic system is defined by the I-V generation and load curves intersection. For understanding how it occurs, firstly considerer a PV module supplying a resistive load, as depicts Figure 8.
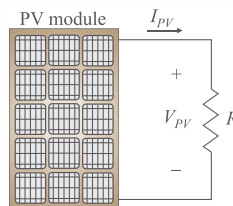

Figure 8. PV module supplying a resistive load.

The load curve is accomplished by the Ohm's Law, in accordance with (6), while the generation curve is related to the PV I-V curve. Both curves are represented at Figure 9.
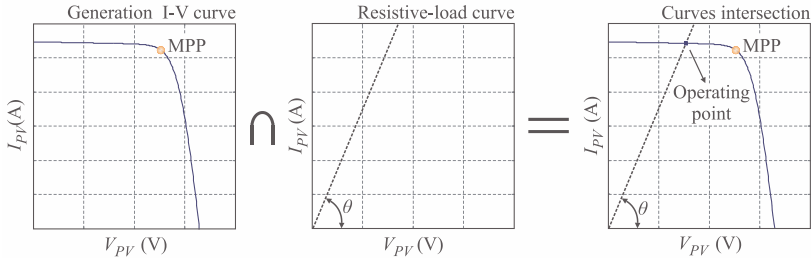
$$I_{PV} = \frac{V_{PV}}{R} \tag{6}$$

Figure 9. Definition of the system operating point by the I-V and load curves intersection.

Even when the load resistance is chosen for both curves intercept each other exactly on the MPP, it is impossible to ensure the maximum power transfer for long time intervals, once when solar radiation or temperature change, the MPP is relocated on the I-V plan.

For solving this problem, in order to maintain the system always operating on the MPP, the load curve should be modified according to solar radiation or temperature changes. For example, from Figure 10, if the PV generation curve is *I-V 1* and the load curve is *Load 1*, the system operating point is given by *MPP 1*. Now, considering a solar radiation and temperature change, the generation curve comes from *I-V 1* to *I-V 2*. In this situation, keeping the same load curve (*Load 1*), the system operating point is established at *X2*, i.e., out of the MPP. However, if the load curve is modified from *Load 1* to *Load 2*, the system backs to operate on the MPP, in this case, *MPP 2*.
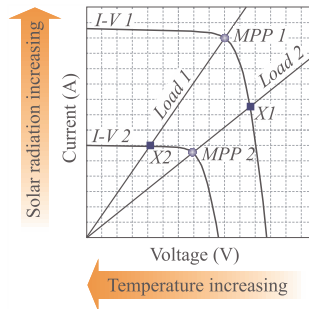

Figure 10. I-V and load curves intersection for defining the PV system operating point.

Evidently, modifying the load curve in accordance with the solar radiation and temperature changes is not a suitable solution, since the load is defined by the user. Nevertheless, if a dc-dc converter is interposed between the PV module and the load, it is possible to control the

converter duty cycle in order to emulate a variable load from the PV terminals point of view, even when a fixed load is employed. The arrangement presented at Figure 11, composed by a PV module, a dc-dc converter and a load, defines the hardware of a maximum power point tracking system.
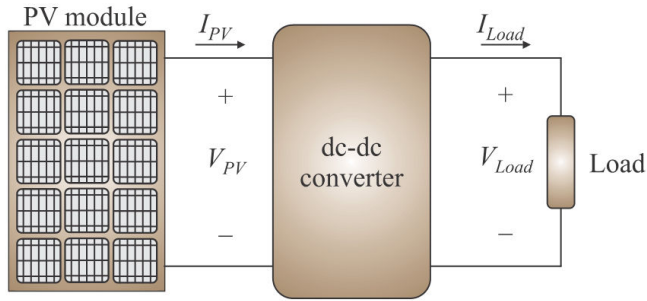

Figure 11. Maximum point tracker system.

It is important to emphasize that the tracking system will present distinct behaviours depending on the dc-dc converter and load-type features. Here, buck, buck-boost, boost, Cuk, SEPIC and zeta converters will be analyzed in association with resistive or constant voltage loads-type.

3.1.1. Analysis for resistive load-type

When a resistive load is connected to the dc-dc converter, Figure 11 may be redrawn as per Figure 12 and equation (7) can be derived.
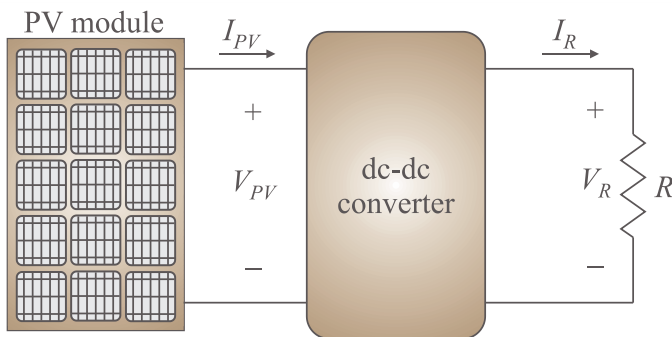

Figure 12. MPPT supplying a resistive load-type.

$$V_R = R I_R \tag{7}$$

Taking into account a literal dc-dc converters static gain G, the input system variables (V_{PV} and I_{PV}) can strictly be associated to the output ones (V_R and I_R), through (8) and (9).

$$G = \frac{V_R}{V_{PV}} \tag{8}$$

$$G = \frac{I_{PV}}{I_R} \tag{9}$$

Isolating V_R in (8) and I_R in (9) and substituting the found results into (7), it is possible to obtain (10).

$$\frac{V_{PV}}{I_{PV}} = \frac{R}{G^2} \tag{10}$$

The term V_{PV}/I_{PV} describes the effective resistance R_{eff} obtained from the PV module terminals. In other words, the dc-dc converter emulates a variable resistance, whose value can be modulated in function of the converter static gain G. This conclusion allows redesigning Figure 12 as Figure 13 and writes (11).
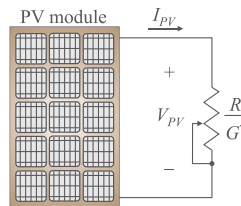

Figure 13. Effective resistance obtained from the PV module terminals.

$$V_{PV} = \frac{R}{G^2} I_{PV} \tag{11}$$

When plotted on the I-V plan, equation (11) results in a straight line whose inclination angle θ, given by 12, is modified according to the converter static gain G.

$$\theta = \mathrm{atan}\left(\frac{G^2}{R}\right) \tag{12}$$

Table 2 presents static gain, as a function of the duty cycle *D*, for the dc-dc converter cregarded in this chapter, for operation in continuous conduction mode (CCM). Applying the results from Table 2 in (12), it is possible to describe the effective inclination angle θ, for each converter, as a variable dependent on the duty cycle *D*, as consequence, Table 3 is obtained.

Power dc-dc converter	Static Gain
Buck	$G = D$
Boost	$G = \frac{1}{1-D}$
Buck-boost, Cuk, SEPIC and zeta	$G = \frac{D}{1-D}$

Table 2. Static gain for some dc-dc converters in CCM.

Power dc-dc converter	Effective load inclination angle θ
Buck	$\theta = atan\left(\frac{D^2}{R}\right)$
Boost	$\theta = atan\left[\frac{1}{(1-D)^2 R}\right]$
Buck-boost, Cuk, SEPIC and zeta	$\theta = atan\left[\frac{D^2}{(1-D)^2 R}\right]$

Table 3. Load curve inclination angle as a function of the converter duty cycle *D*.

Theoretically, since the duty cycle is limited between 0 and 1, the effective inclination angle becomes restricted into a range whose extremes are dependent on the considered dc-dc converter. For instance, when buck converter is taken into account, for null duty cycle, *D*=0, (13) is found.

$$\theta\,\big|_{D=0} = atan\left(\frac{0^2}{R}\right) = 0 \tag{13}$$

Thereby, if the duty cycle is set on its high value, *D*=1, (14) may be written.

$$\theta\,\big|_{D=1} = atan\left(\frac{1}{R}\right) \tag{14}$$

In other to extend the presented analysis for further converters, a similar procedure may be applied, resulting at Table 4 and Figure 14.

From Table 4 it is noticed that effective load inclination angle defines an area on the I-V plan where the maximum power can be tracked. For a better understanding, Table 4 is graphically explained through Figure 14, from where two distinct regions are identified: tracking and non tracking regions.

The tracking region refers to the area on the I-V plan in which the dc-dc converter is able to emulate a proper effective load curve in order to intercept the I-V curve exactly on the MPP, ensuring the maximum power transfer. Note, when solar radiation or temperature change, the maximum power point is relocated on the I-V plan, thus, the effective load inclination angle must also be modified in order to reestablish the maximum power transfer. However, this condition is only suitable if the MPP is located inside the tracking region, otherwise, the system operating point will be set out of the MPP.

Power dc-dc converter	Minimum effective load inclination angle	Maximum effective load inclination angle
Buck	$\theta\big|_{D=0}=0$	$\theta\big|_{D=1}=atan\left(\frac{1}{R}\right)$
Boost	$\theta\big|_{D=0}=atan\left(\frac{1}{R}\right)$	$\theta\big|_{D=1}=90°$
Buck-boost, Cuk, SEPIC and zeta	$\theta\big|_{D=0}=0$	$\theta\big|_{D=1}=90°$

Table 4. Minimum and maximum effective load inclination for some dc-dc converters.
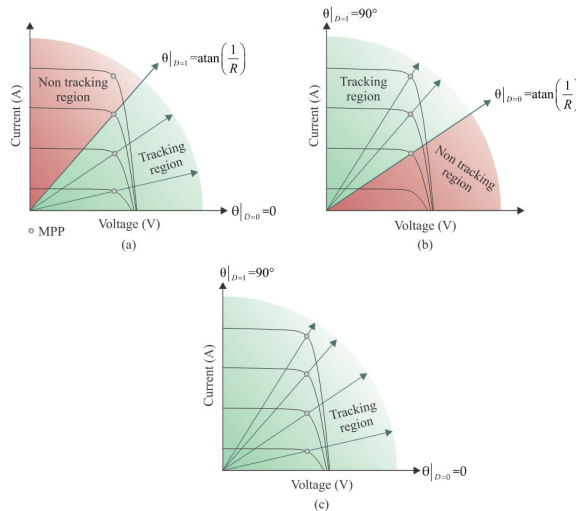

Figure 14. Tracking and non tracking regions for: (a) buck converter; (b) boost converter and (c) buck-boost, Cuk, SEPIC and zeta converters.

Comparing the graphical results, it is verified that buck-boost, Cuk, SEPIC and zeta are the most appropriated converters for maximum power point tracking applications, once they may track the MPP independently on its position on the I-V plan. On the other hand, buck

and boost converters are not indicate for this proposal, since their tracking area is only a part of the whole I-V plan. In order to validate the proposed theory, buck, boost and buck-boost converters were designed and assembled in laboratory, according to Figure 15.
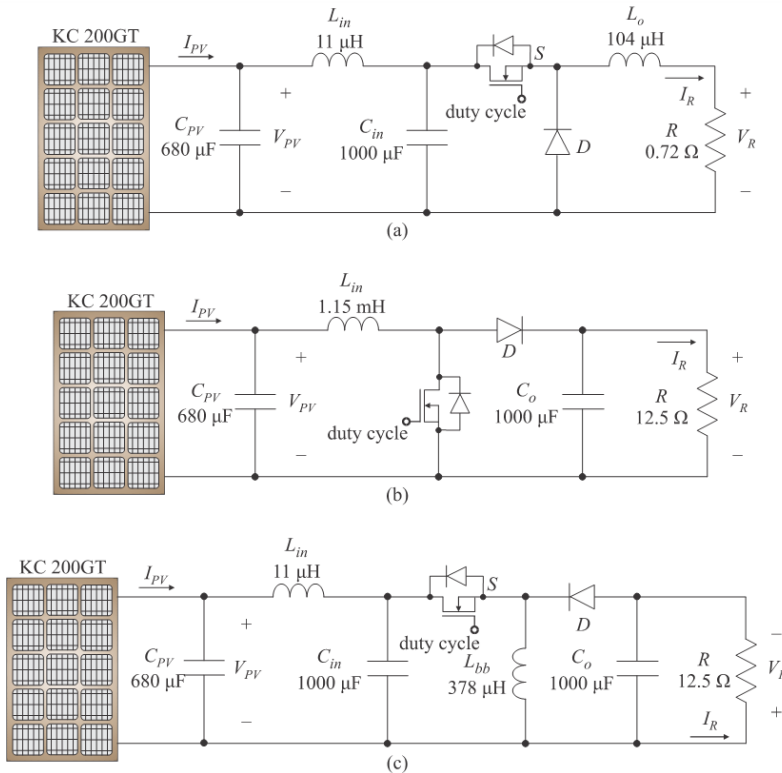

Figure 15. a) buck, (b) boost and (c) buck-boost power stage converters.

For achieving the experimental tests, the converters duty cycle was linearly varied from 0 to 1, while PV voltage and current were measured. By the use of a scope on XY mode, the I-V curve was traced, and the found results are shown at Figure 16.

Notice that I-V curve is partially plotted on the I-V plan when buck and boost converters are regarded, and on the whole I-V plan, when buck-boost converter is considered. Additionally, the area in which the I-V curves were traced is in accordance with the tracking region, theoretically defined for each converter, validating the analysis.

On the next subsection, the resistive load will be replaced by a constant voltage load-type. This analysis is relevant and mandatory, since in many applications, PV systems are employed in battery charges, or even, delivering power to a regulated dc bus.

3.1.2. Analysis for constant voltage load-type

The analysis concerning to dc-dc converters operating as MPPT when a constant voltage load-type is considered follows the same procedures presented for resistive loads. For beginning, consider the MPPT system shown in Figure 17, in which a dc voltage source is supplied by a PV module through a literal dc-dc converter.
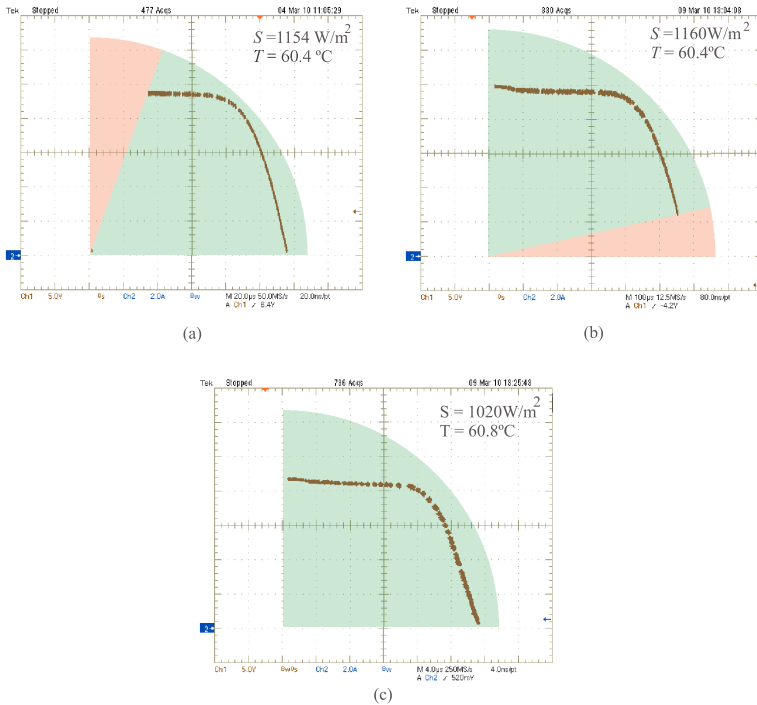

Figure 16. Experimental results for (a) buck, (b) boost and (c) buck-boost converters.
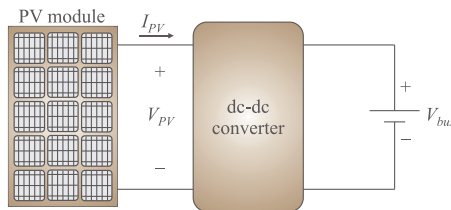

Figure 17. MPPT supplying a constant voltage load-type.

In this case, the output converter voltage is imposed by the load, permitting to write (15) and to model both, dc-dc converter and voltage load, as a controlled voltage source, as is shown in Figure 18.
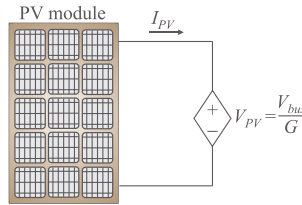
$$V_{PV} = \frac{V_{bus}}{G} \qquad (15)$$

Figure 18. Equivalent MPPT system obtained from the PV module terminals.

Taking into account the static gain G presented at Table 2, it is possible to define the equivalent voltage source for each dc-dc converter as a function of the duty cycle D, resulting on Table 5. Due to the duty cycle range restriction, $0<D<1$, the voltage imposed by the equivalent controlled voltage source across the PV module terminals is also limited. For example, when buck converter is regarded, equations (16) and (17) are obtained from the first line of Table 5, describing the system behavior for $D=0$ and $D=1$, respectively.

Power dc-dc converter	Equivalent voltage source value
Buck	$V_{PV} = \frac{V_{bus}}{D}$
Boost	$V_{PV} = (1-D)V_{bus}$
Buck-boost, Cuk, SEPIC and Zeta	$V_{PV} = \frac{(1-D)}{D}V_{bus}$

Table 5. Minimum and maximum effective load inclination for some dc-dc converters.

$$V_{PV}\big|_{D=0} = \frac{V_{bus}}{0} \rightarrow \infty \qquad (16)$$

$$V_{PV}\big|_{D=1} = V_{bus} \qquad (17)$$

It is important to emphasize that the maximum voltage across the PV module terminals is its open circuit voltage, thus, the minimum duty cycle value must be defined in order to satisfy this condition. From the exposed, (16) is replaced by (18).

$$V_{PV}\big|_{D=D_{\min}} = \frac{V_{bus}}{D_{\min}} = V_{oc} \tag{18}$$

Extending the analysis for further converters, Table 6 is obtained.

The graphical representation allows understanding how the dc-dc converter feature impacts on the tracking quality when constant voltage loads are employed, as depicts Figure 19. When the maximum power point is located inside the tracking region, the dc-dc converter may apply on the PV output terminals a voltage value for ensuring its operation on the MPP. Otherwise, even when the better tracking algorithm is used, there is no possible to track it.

Power dc-dc converter	Minimum voltage across the PV module terminals	Maximum voltage across the PV module terminals
Buck	$V_{PV}\big|_{D=1} = V_{bus}$	$V_{PV}\big|_{D=D_{min}} = V_{oc}$
Boost	$V_{PV}\big|_{D=1} = 0\,V$	$V_{PV}\big|_{D=0} = V_{bus}$
Buck-boost, Cuk, SEPIC and zeta	$V_{PV}\big|_{D=1} = 0\,V$	$V_{PV}\big|_{D=D_{min}} = V_{oc}$

Table 6. Minimum and maximum voltage values across the PV module terminals.
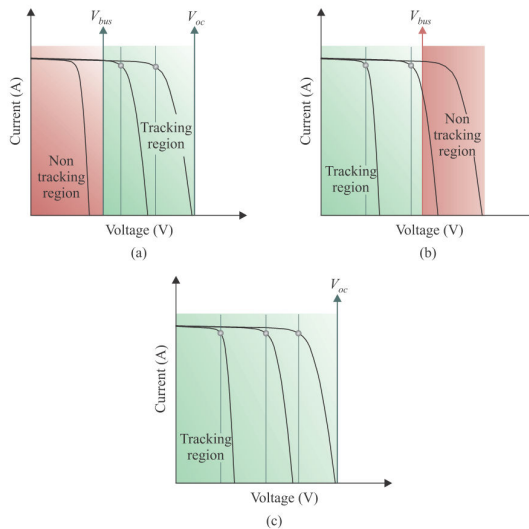

Figure 19. Tracking and non tracking regions for: (a) buck converter; (b) boost converter and (c) buck-boost, Cuk, SEPIC and zeta converters.

In addition, notice that temperature changes may directly affect the tracking quality: commonly, PV systems are designed considering its operation on the SCT, i.e., $T = 25°$, however, when PV modules are exposed to the solar radiation, its real temperature of operation encreases and, as consequence, the voltage associated to MPP is moved to the left. This behavior is critical for buck converter, as per Figure 19 (a), since its non tracking region is also on left of V_{bus}.

Although boost converter also presents a non tracking region, in this case it presents a proper tracking behavior, once temperature increasing replaces the MPP to left, toward to the tracking region, in according to Figure 19 (b).

Finally, buck-boost converter (and similars) can track the MPP independent on its position on the I-V pan, as is shown on Figure 19 (c). Furthemore, these converters are also indicated for tracking applications, when constant voltage loads are employed.

3.2. MPPT from the tracking algorithm point of view

The tracking algorithm performance is fundamental for an efficient tracking response. Usually, the algorithm receives the PV module voltage and current as input data and defines the dc-dc converter duty cycle that establishes the system operating point on the MPP, as depicts Figure 20.
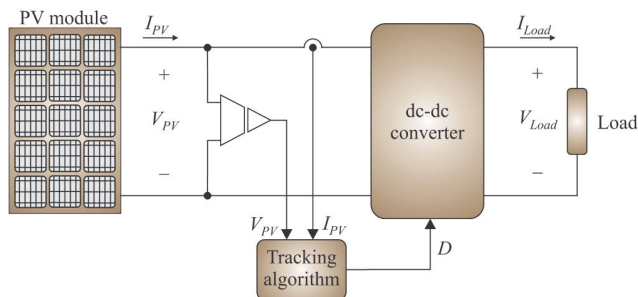

Figure 20. Typical input and output data related to MPPT algorithms.

As the radiation and temperature are dynamic variables, and the MPP depends on both of them, the algorithm must practically work in real time, updating the duty cycle for a fast and accurate tracking.

On the literature, there are several proposed algorithms for improving the tracking speed, accuracy or both, but the algorithm efficiency is directly associated to the complexity of implementation.

In this section, based on the PV curves understanding, a new tracking method is developed, whose main characteristics are: simplicity, excellent tracking dynamic, accuracy, stability in steady-state (no oscillations), and low cost.

Before presenting this proposal, a review of the most commonly employed MPPT algorithms is presented, where Constant Voltage, Perturb and Observe (P&O) and Incremental Conductance (IncCond are briefly discussed.

3.2.1. Constant Voltage

This method is achieved in or to impose the voltage across the PV terminals clamped at a fixed value, normally specified to ensure the maximum power transfer on the STC [4]. Once a single voltage sensor is needed, it is featured by simplicy of implementation and low cost, but for any temperature change, the PV operating point is set out of the MPP.

3.2.2. Perturb and Observe

Perturb and Observe (P&O) is one of the most diffused MPPT algorithms, whose tracking response is independent on the environmental conditions, however, its implementation requires a voltage and a current sensor, increasing the cost and complexity [11].

When in operation, the P&O algorithm calculates the PV output power and perturbs the converter duty cycle (increasing or decreasing it). After perturbation, the PV output power is recalculated and, if it was increased, the perturbation is repeated on the same direction, otherwise, it is inverted.

The main drawbacks associated to this method are the oscillation in steady-state, due to the constant perturbations, the slow tracking dynamic and the inability to proper operate during fast changes of solar radiation.

3.2.3. Incremental Conductance

The Incremental Conductance (IncCond) method is featured for combining both, tracking speed and accuracy [13]. From the voltage V_{PV} and current I_{PV} measurements, the algorithm calculates the photovoltaic output power P_{PV} and its derivative in function of the voltage dP_{PV}/dV_{PV}, using both results to define if the duty cycle must be increased or decreased, in order to impose the system operating point on the MPP. Usually the IncCond method is implemented digitally, and the derivative is calculated by the microcontroller according to (19).

$$\frac{dP_{PV}}{dV_{PV}} = I_{PV}(n) + V_{PV}(n)\frac{I_{PV}(n-1)-I_{PV}(n)}{V_{PV}(n-1)-V_{PV}(n)} \tag{19}$$

From (19), the following decision logic is achieved:

a. if $dP_{PV}/dV_{PV}\,0$ (left of MPP), the duty cycle is changed for elevating the PV module voltage;

b. if $dP_{PV}/dV_{PV}\,0$ (right of MPP), the duty cycle is altered for decreasing the output voltage;

c.   if $dP_{PV}/dV_{PV} = 0$ (at MPP), the duty cycle is maintained unchangeable.

This tecnique is characterized for presenting high tracking speed (variabe step) and accuracy (no oscillation), however, it is more complexy than P&O, once the derivative must be calculated in real time and also require a voltage and a current sensor.

3.2.4. A MPPT algorithm based on temperature measurement

The MPPT algorithm based on temperature measurement, named by MPPT-temp [22], consists on the unification of simplicity related to Constant Voltage method with the velocity and accuracy tracking related to the Incremental Conductance technique.

The development of this method comes from (3), rewritten in (20). Note that the voltage in which the maximum power is established depends exclusively on the PV surface temperature. Thereby, accomplishing the temperature measurement, the maximum power voltage V_{mpp} may be determined and actively imposed across the PV terminals in real time. The configuration needed for implementation of this new method is depicted at Figure 21.

$$V_{mpp} = V_{mpp}^{STC} + \left(T - T^{STC}\right)\mu_V \tag{20}$$
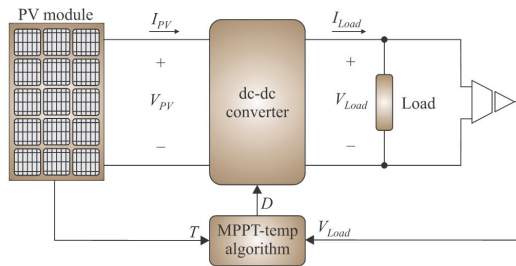

Figure 21. Configuration of the new tracking method.

The following steps describe how the maximum power point is achieved by the proposed method:

1.   The PV module surface temperature T and the load volatge V_{Load} are measured by a temperature sensor and a volatge sensor, respectivelly;

2.   Both sinals are applyed as input data for the tracking algorithm, whose output is the dc-dc converter static gain G_{mpp}, in acordance with (21);

$$G_{mpp} = \frac{V_{Load}}{V_{mpp}^{STC} + \left(T - T^{STC}\right)\mu_V} \tag{21}$$

3.Defining the dc-dc converter, an expression for determine the duty cycle may be derived. For example, considering a buck converter, i.e. *G=D*, the maximum power point is acomplished when (21) is rewritten as (22).

$$D_{mpp} = \frac{V_{Load}}{V_{mpp}^{STC} + (T - T^{STC})\mu_V}$$
(22)

For extending the analisys, Table 7 present the equitions employed by the tracking algorithm to calculate the duty cycle that imposes the PV operating point on the MPP.

Power dc-dc converter	Duty cycle for operation on the MPP
Buck	$D_{mpp} = \frac{V_{Load}}{V_{mpp}^{STC} + (T - T^{STC})\mu_V}$
Boost	$D_{mpp} = 1 - \frac{V_{Load}}{V_{mpp}^{STC} + (T - T^{STC})\mu_V}$
Buck-boost, Cuk, SEPIC and zeta	$D_{mpp} = \frac{V_{Load}}{V_{Load} + V_{mpp}^{STC} + (T - T^{STC})\mu_V}$

Table 7. Duty cycle for maximum power point operation.

Table 7 evidences the simplicity of the proposed method: from the temperature measurement it is possible directly set the duty cycle, ensuring the maximum power transfer from the PV module to the load. Additionally, there is no need computational requirements, recursive procedures and, due to the slow dynamic associated to the temperature changes, the tracking is smooth, stable and occurs in real time, for any combination of solar radiation and temperature.

It is important to emphasize the restrictions associated to the dc-dc converter, as it was previously studied at last section, may imply in a poor tracking quality, even when the MPPT-temp method is employed. In order to finalize the chapter, the results obtained from an experimental prototype are presented.

The prototype was implemented for processing the power generated by a KC200GT PV module, from Kyocera, whose electrical specifications are listed at Table 1. A dc-dc buck-boost converter was chosen for composing the hardware, because of its proper tracking behavior. Consequently, the equation to define the duty cycle is given by (23).

$$D_{mpp} = \frac{V_{Load}}{V_{Load} + V_{mpp}^{STC} + (T - T^{STC})\mu_V} = \frac{V_{Load}}{V_{Load} + 29.8 - 0.14T}$$
(23)

For measuring the PV module surface temperature, a precision centigrade temperature sensor (LM35) was used. This device presents a linear gain of 10 mV/°C. Furthermore, in order to execute the tracking algorithm, a simple PIC 18F1320 microcontroller was employed.

The tracking method validation was achieved plotting the PV operating point on the I-V plan during temperature and solar radiation changes, as is illustrated in Figure 22. For reaching this result a scope on XY mode, where X refers to the PV output voltage and Y refers to the PV output current, was employed.
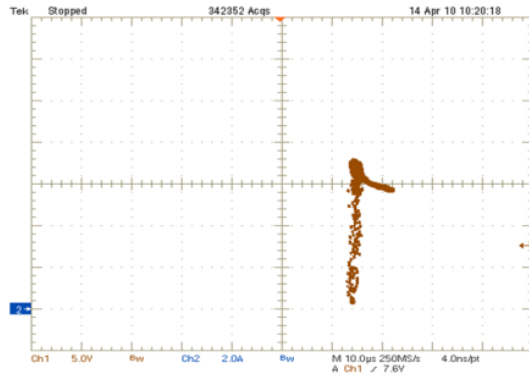

Figure 22. Experimental PV operating point on I-V plan during temperature and solar radiation changes. Scope on XY mode (X-voltage, Y-current)
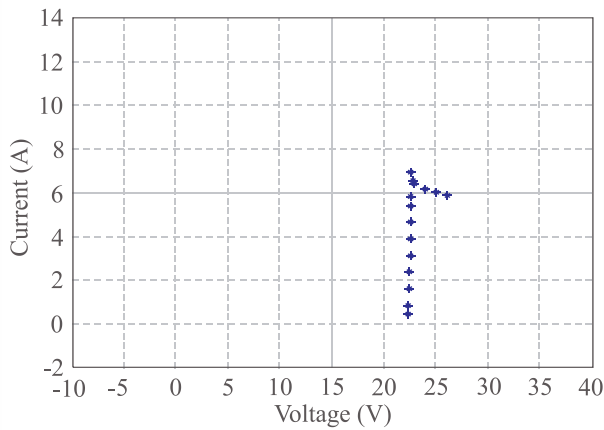

Figure 23. Theoretical MPP trajectory for solar radiation and temperature measured during experimental evaluation.

In order to prove that the obtained experimental trajectory coincides with the MPP, the values of solar radiation and temperature were also collected by a data logger and summarized by Table 8. The measurements were achieved on middle of April in the Florianopolis Island – south of Brazil – located at latitude 27°.

Solar radiation	Temperature
900 W/m^2	51°C
850W/m^2	50°C
830W/m^2	49°C
802W/m^2	41°C
787W/m^2	34°C
770W/m^2	26°C
700W/m^2	51°C
600W/m^2	51°C
500W/m^2	51°C
400W/m^2	51°C
300W/m^2	52°C
200W/m^2	52°C
100W/m^2	53°C
50W/m^2	53°C

Table 8. Solar radiation and temperature values obtained from data logger during experimental tests.

From Table 8, and employing (3) and (4), the theoretical voltage and current values for the system operating on the MPP were determined and plotted on the I-V plan, resulting at Figure 23, from where it is possible to conclude that the trajectory obtained by experimentation is equivalent to the trajectory described by the maximum power point.

4. Conclusion

Currently the most common employed PV tracking algorithm are Perturb and Observe and Incremental Conductance. Perturb and observe is simple, however it failures to track the MPP under abrupt changes on solar radiation and presents oscillations around the MPP on steady-state. Incremental conductance is accurate, however, it implementation is more complex. In these both algorithms, it is necessary to measure the PV output voltage and current.

The proposed algorithm is simpler than perturb and observe and more accurate than the incremental conductance. Furthermore, the current sensor is substituted by a temperature sensor, implying in cost reduction. Eliminating the current sensor means avoid the output power high frequency variation associated to the PV current (directly proportional to solar radiation), thus, there is no oscillation around the MPP. Since the tracking is based on the temperature, its low dynamic ensures a soft tracking, but accurate and fast.

Based on the exposed, this tracking method employment allows a significant improvement on the PV operation. Note that in PV generation the power losses may be separated in two terms: the first one is associated to the power converters efficiency and the second to the tracking algorithm efficiency. Thus, if an optimized tracking algorithm is employed, the global efficiency is increased.

From the dc-dc analysis it was verified that buck and boost converters, even been largely applied for tracking applications, are not proper for this proposal, since they can track the MPP only in a part of the I-V plan. On the other hand, buck-boost converter (and Cuk, SEP-IC or zeta) may track the MPP around the whole I-V plan, configuring the better option for tracking applications.

Finally, an optimized tracking system only is obtained if both, dc-dc converter and tracking algorithm properly operate. This condition is accomplished when a buck-boost converter is employed in combination with the MPP-temp tracking method.

Acknowledgements

Author details

Roberto Francisco Coelho[*] and Denizar Cruz Martins

*Address all correspondence to: roberto@inep.ufsc.br

Federal University of Santa Catarina - Electrical Engineer DepartmentPower Electronics Institute, Florianópolis, Brazil

References

[1] Jung-Min, K., Kwang-Hee, N., & Bong-Hwan, K. (2006). Photovoltaic Power Conditioning System With Line Connection.IEEE. *Transactions on Industrial Electronics*, 53, 1048-1054.

[2] De Souza, K. C. A., dos Santos, W. M., & Martins, D. C. (2010). Active and reactive power control for a single-phase grid-connected PV system with optimization of the ferrite core volume. *IEEE/IAS International Conference on Industry Applications (INDUSCON)*, 1-6.

[3] Ciobotaru, M., Teodorescu, R., & Blaabjerg, F. Control of single-stage single-phase PV inverter. *European Conference on Power Electronics and Applications*, 10.

[4] Ghaisari, J., Habibi, M., & Bakhsahi, A. (2007). An MPPT Controller Design for Photovoltaic (PV) System Based on the Optimal Voltage Factor Tracking. *IEEE Canada electrical Power Conference*, 359-362.

[5] Pandey, A., Dasgupta, N., & Mukerjee, A. K. (2007). A Single-Sensor MPPT Solution. *IEEE Transaction on Power Eletronics*, 22(2), 698-700.

[6] Sokolov, M., & Shmilovitz, D. (2008). A modified MPPT Scheme for Accelerate Convergence. *IEEE Transactions on Energy Conversion*, 23(4), 1105-1107.

[7] Villalva, M. G., & Ruppert, E. F. (2009). Analysis and Simulation of the P&O MPPT Algorithm Using a Linearized PV Array Model. *10th Brazilian Power Electronics Conference*, 231-236.

[8] Aranda, E. D., Galán, J. A. G., Cardona, C. S., & Marques, J. M. A. (2010). Measuring the I-V Curve of PV Generator. *IEE Industrial Electronics Magazine*, 3(3), 4-14.

[9] Coelho, R. F., Concer, F. M., & Martins, D. (2009). *A Study of the Basic DC-DC converters Applied in Maximum Power Point Tracking. 10th Brazilian Power Electronics Conference*, 673-667.

[10] Hohm, D. P., & Ropp, M. E. (2000). Comparative Study of Maximum Power Point Tracking Algorithms Using an Experimental, Programmable, Maximum Power Point Test Bed. *IEEE Photovoltaic Specialists Conference*, 1699-1702.

[11] Tan, C. W., Green, T. C., & Hernandez-Aramburo, C. A. (2008). Analysis of Perturb and Observe Maximum Power Point Tracker Algorithm for Photovoltaic Applications. *IEEE 2nd International Power and Energy Conference*, 237-242.

[12] Boico, F., & Lahman, B. (2006). Study of Different Implementation Approaches for a Maximum power Point Tracker. *IEEE Computers in Power Electronics*, 15-21.

[13] Liu, B., Duan, S., Liu, F., & Xu, P. (2007). Analysis and Improvement of a Maximum Power Point Tracking Algorithm Base on Incremental Conductance Method for Photovoltaic Array. *IEEE International Conference on Power Applications*, 637-641.

[14] Yuvarajan, S., & Shoeb, J. (2008). A Fast and Accurate Maximum Power Point Tracker for PV Systems. *IEEE Applied Power Electronics Conference and Exposition*, 167-172.

[15] Femia, N., Petrone, G., Spagnuolo, G., & Vitelli, M. (2004). Optimizing Sampling Rate of P&O MPPT Technique. *IEEE Power Electronics Specialist Conference,*, 3, 1945-1949.

[16] Pandey, A., Dasgupta, N., & Mukerjee, A. (2006). Designe Issues in Implementing MPPT for Improved Tracking and Dynamic Performance. *IEEE Conference on Industrial Electronics*, 4387-4391.

[17] Onat, Nevzat. (2010). Rececent developments in maximum power point tracking technologies for photovoltaic systems. *International Journal of Photoenergy*.

[18] De Brito, M. A. G., Junior, L. G., Sampaio, L. P., Melo, G. A., & Canesin, C. A. (2011). Main maximum power point tracking strategies intended for photovoltaics. *XI Power Electronics Brazilian Conference*, 524-530.

[19] Integration of alternative sources of Energy. (2006). Felix A. Ferret and M. Godoy Simões. Wiley-Intercience. *IEEE Press, New Jersey*.

[20] http://www.physicalgeography.net/fundamentals/7f.html.

[21] Coelho, R. F., Concer, F. M., & Martins, D. (2009). A Proposed Photovoltaic Module and Array Mathematical Modelling Destined to Simulation. *IEEE International Symposium on Industrial Electronics*, 1624-1629.

[22] Coelho, R. F., Concer, F. M., & Martins, D. C. (2010). A MPPT approach based on temperature measurements applied in PV systems. *IEEE/IAS International Conference on Industry Applications*, 1-6.